Electronic supplementary information (ESI)

# Multifunctional covalent organic framework with extended π-d conjugated structure for lithium-sulfur batteries

*Manman Wu[a,b], Hao Zhang[a], Shaobo Cai[a], Xiandi Ma[a], Menggai Jiao[a], Yongzheng Fang[a,c], Yiyang Liu[a,*], Zhen Zhou[a,d,*]*

[a] Interdisciplinary Research Center for Sustainable Energy Science and Engineering (IRC4SE$^2$), School of Chemical Engineering, Zhengzhou University, Zhengzhou 450001, China.

[b] Key Laboratory of Advanced Energy Materials Chemistry (Ministry of Education), College of Chemistry, Nankai University, Tianjin 300071, China.

[c] Longmen Laboratory, Luoyang 471023, Henan, China.

[d] School of Materials Science and Engineering, Institute of New Energy Material Chemistry, Renewable Energy Conversion and Storage Center, Nankai University, Tianjin 300350, China.

E-mail: liuyiyang@zzu.edu.cn (Y.Y.L); zhouzhen@nankai.edu.cn (Z.Z.)

**Keywords**: covalent organic frameworks, lithium-sulfur batteries, conjugated structure, separator modification

## 1. Experimental Section

### Materials

2,5-dihydroxyterephthalaldehyde (HBC, 99.72%) and Nickel acetate tetrahydrate ($NiOAc.4H_2O$, 98%) and sulfur power (S) were purchased from Aladdin Co., Ltd. 2,3,5,6-tetraaminobenzoquinone (TABQ, 97%) was provided by Jilin Chinese Academy of Sciences-Yanshen Technology Co., Ltd. N-Methylpyrrolidone (NMP), N, N-dimethylformamide (DMF) and methanol (MeOH, AR) were obtained by Sinopharm Chemical Reagent Co., Ltd. Poly(1,1-difluoroethylene) (PVDF) and electrolytes were provided by Suzhou Duoduo Chemical Technology Co. Ltd. Super P (SP) was purchased from Shenzhen Kejingzhida Technology Co., Ltd. All chemicals were used without further purification.

**Synthesis of Ni-COF**

HBC (166 mg, 1 mmol) and TABQ (84 mg, 0.5 mmol), excess nickel acetate, and 10 mL dried NMP were added to a 25 mL glass bottle. The resulting solution was sonicated for half an hour to obtain a homogenous dispersion. The glass bottle was transferred into a 25 mL Teflon-lined stainless-steel autoclave. The autoclave was subsequently sealed and heated at 120 ºC for three days. After cooling to room temperature, the generating black precipitate was collected by filtration and washed with DMF and MeOH several times. Finally, the precipitate was dried under vacuum at 80 ºC overnight to obtain Ni-COF.

**Preparation of Ni-COF@PP separator**

The Ni-COF@PP separator was prepared by coating the Ni-COF slurry on one side of the PP separator (Celgard 2500). The Ni-COF slurry was prepared by mixing Ni-COF (40 wt%), Super P (40 wt%) and PVDF (20 wt%) in NMP. The slurry was ground well and then coated on the PP separator. The composite separator was dried at 50 °C for 12 hours, followed by cutting into discs with a diameter of 16 mm.

**Preparation of S@SP cathode**

The S@SP composite was prepared using a melt-diffusion method. Sulfur (70 wt%) and Super P (SP, 30 wt%) were mixed and ground in mortar, then heated at 155°C for 12 hours. The resulting S@SP was combined with SP, and PVDF in an 8:1:1 weight ratio. Then the mixture was ground while gradually adding NMP to form a slurry. This slurry was coated onto carbon-coated Al foil and dried in a vacuum oven at 60°C for 24 hours. The electrode was then cut into 12 mm diameter discs and further dried at 60°C, resulting in the final S@SP cathode with a sulfur loading of approximately 1.5 mg $cm^{-2}$.

**Coin cell fabrication and electrochemical measurements**

The CR2032 coin-type Li-S batteries were assembled in an Ar-filled glovebox ($O_2$ < 0.1 ppm, $H_2O$ < 0.1 ppm) with lithium foils as the counter and reference electrodes,

the as-prepared S@SP cathode as working electrodes. The electrolyte was 1M 1.0 M LiTFSI (DOL: DME=1/1) with 0.1 M $LiNO_3$ as an additive. The electrolyte/sulfur ratio for this work is 11.80 μL mg-1. The Ni-COF@PP separator and the commercial PP were used as separators, respectively. Galvanostatic charge/discharge measurements were performed on a LAND CT2001A testing system with a voltage window of 1.7−2.8 V under various C-rates (1 C = 1672 mAh $g^{-1}$). The Solartron analytical 1400 cell test system was used to collect the cyclic voltammetry (CV) curves. Electrochemical impedance spectroscopy (EIS) was conducted over the frequency ranging from 0.1-10 k Hz at a 10 mV.

**Li || Li symmetric cells assembly**

All Li–Li symmetric cells were assembled in an Argon-filled glove box (< 1 ppm of $O_2$ and $H_2O$). The electrolyte was kept in line with those of conventional Li-S batteries, ensuring a controlled total volume of 30 μL. The Ni-COF@PP separator and the commercial PP were used as separators, respectively.

**2. Material Characterizations**

Powder X-ray diffraction (PXRD) of the samples were collected through Rigaku B/Max-RB diffractometer with a Cu-Kα radiation source (λ= 0.154 nm). Fourier transform infrared (FTIR) spectra of the samples were measured on a BRUKER INVENI0 with a resolution of 2 cm-1 in the spectral range of 4000 to 400 cm-1. Solid-state $^{13}C$ nuclear magnetic resonance (NMR) were performed using a Bruker Avance Neo 400WB. Nitrogen adsorption-desorption measurements were conducted on Micromeritics ASAP 2460 physisorption apparatus at 77K. X-ray photoelectron spectroscopy (XPS) measurements were performed by Shimadzu/Krayos AXIS Ultra DLD. Field emission scanning electron microscopy (SEM) was conducted using a JSM-6390 microscope from JEOL. Transmission electron microscopy (TEM) was carried out on FEI Talos-F200S. Ni K-edge X-ray absorption fine structure (XAFS) measurements were obtained at 4B9A beamline of Beijing Synchrotron Radiation Facility (BSRF). ICP measurement was conducted using Shimadzu ICPE-9820. UV-

vis spectroscopy was measured by Shimadzu UV-2700i. The electrical conductivity of Ni-COF was measured by a four-point probe method at room temperature (~ 298 K).

## 3. Electrochemical Measurements

### Ion conductivity measurement

The ionic conductivity ($\sigma$) of the electrolyte-soaked separators was evaluated with SS| separator |SS cells by testing the EIS in the frequency range from $10^6$ to 0.01 Hz on the electrochemical workstation. The ionic conductivity is calculated according to the following equation:

$$\sigma = \frac{d}{RS}$$

where $d$ and $S$ are the thickness and effective face area of the separators, respectively, and $R$ is derived from the low intersection of the high frequency semi-circle on a complex impedance plane with the Z axis.

Based on the Arrhenius relationship between ionic conductivity and temperature:

$$In\sigma = In\sigma_0 - \frac{E_a}{RT}$$

where $R$, $T$, $\sigma_0$, and $E_a$ are the gas constant (8.314 J $K^{-1}$ $mol^{-1}$), the absolute temperature and the frequency factor (independent of T), and the activation energy of ion conduction, respectively. The apparent activation energy ($E_a$) of ionic conductivity was calculated according to the following formula:

$$E_a = -b \times R$$

where $b$ is the slope of the straight line obtained from the plot of lnσ against 1000/T.

### Lithium ion transference number ($tLi^+$)

The lithium ion transference number ($tLi^+$) was calculated by chronoamperometry at a constant step potential of 10 mV. Each separator was separately sandwiched between two lithium metal electrodes in a coin type cell (CR2032) and $tLi^+$ was calculated from the ratio of steady state current to initial state current according to the following equation:

$$tLi^{+} = \frac{I_s(\Delta V - I_0 R_0)}{I_0(\Delta V - I_s R_s)}$$

where $R_0$ and $R_s$ refer to the interfacial resistance before and after AC impedance. $I_0$ and $I_s$ represent the current values in the initial and steady states under a polarization potential of 10 mV in the DC process.

**Lithium-ion diffusion coefficient**

The lithium-ion diffusion coefficient $D_{Li^+}$ ($cm^2$ $s^{-1}$) is evaluated by the cyclic voltammetry method and calculated according to the Randles-Sevick equation:

$$I_p = 2.69 \times 10^5 n^{1.5} A D_{Li^+}^{0.5} C_{Li} v^{0.5}$$

where $I_p$ (A) is the peak current value, $n$ represents the number of electrons in the reaction (for Li-S batteries, n = 2), $A$ ($cm^2$) indicates the electrode area, $C_{Li}$ (mol $mL^{-1}$) means the lithium-ion concentration in the electrolyte, and $v$ stands for the scanning rate (V $s^{-1}$).

**$Li_2S_6$ adsorption test**

A 10 mM $Li_2S_6$ solution was obtained by mixing $Li_2S$ and S with a molar ratio of 1:5 in DME solution, stirring for 24 h in the glove box. Subsequently, 100 mg of Ni-COF was added to 10 mL $Li_2S_6$ solution. The blank $Li_2S_6$ solution was used for comparison.

**$Li_2S_6$ symmetric cells test**

A symmetrical cell of Ni-COF was assembled using 20 μL of $Li_2S_6$ catholyte (0.2M $Li_2S_6$ in DOL/DME). The mass loading was around 1 mg $cm^{-2}$. The CV measurement was operated in the electrochemical workstation within -1.0~1.0 V at a scan rate of 5 mV $s^{-1}$.

**$Li_2S$ nucleation measurements**

For the study of liquid-solid conversion kinetics, the material was dissolved in isopropanol and then dropped onto round carbon cloth disks (12 mm), the total mass loading was controlled around 1 mg. The prepared carbon cloth disks and lithium foils were used, respectively, as the cathode and anode to assemble the battery. 25 μL $Li_2S_8$

catholyte (0.2 M $Li_2S_8$, 1 M LiTFSI in tetreglyme) and 25 μL electrolytes without $Li_2S_8$ were added to the cathode and anode sites, respectively. The batteries with Ni-COF-based electrode were first discharged to 2.06 V under a constant current of 0.112 mA and then kept potentiostatically at 2.05V until the current dropped below $10^{-5}$ A. The nucleation capacity of $Li_2S$ can be calculated by the integral area of the plotted curve through Faraday's Law.

**4. Calculation Details**

For the part of density functional theory (DFT) calculations, the geometry optimization was carried out by using the Vienna Ab initio Simulation Package (VASP)[1]. The Perdew-Burke-Ernzerhof (PBE) functional within the generalized gradient approximation (GGA) was employed to describe the electron exchange-correlation energies[2]. The projector augmented wave (PAW) method was used together with a plane-wave basis set expanded to an energy cutoff of 600 eV[3]. The DFT-D3 method was adopted to correct van der Waals interactions[4]. The convergence criterion in geometry optimization was set to $10^{-5}$ eV for energy and 0.05 eV $Å^{-1}$ for forces, respectively. The x and y directions were set parallel to the Ni-COF plane, while the z direction was set perpendicular to the Ni-COF plane. A vacuum layer of 20 Å along the z direction was included to prevent the interaction between periodic images. The k-points sampling of Brillouin zone was performed by using a Monkhorst-Pack grid[5] of 3×3×1 and 6×6×1 for geometry optimizations and electronic structure computations, respectively.

Geometry optimizations without symmetry restriction were performed using the B3LYP hybrid density functional[6], as implemented in the Gaussian 09 suite of programs[7]. The self-consistency field energy, total energy, and force threshold values were set as defaults within the program.

## 5. Supporting Figures

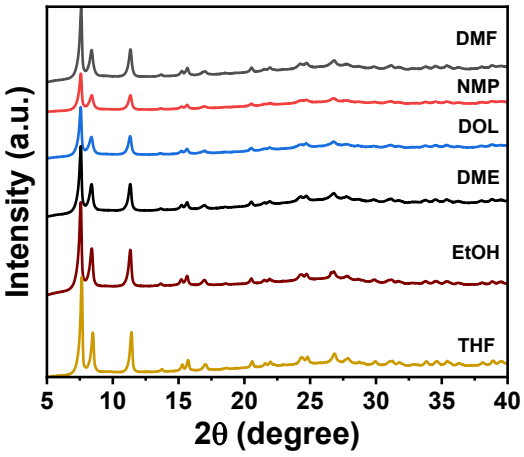


Figure S1. PXRD patterns of Ni-COF after soaking in different solutions for 72 h.

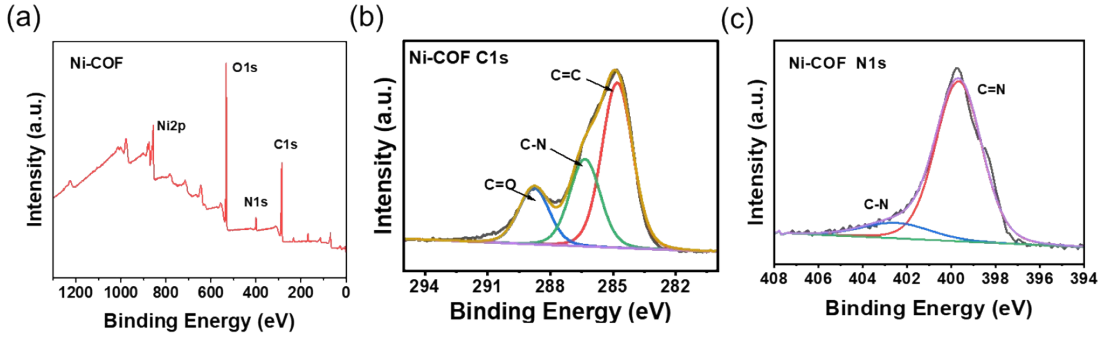


Figure S2. (a) XPS full spectrum of Ni-COF. (b) High-resolution C 1s XPS of Ni-COF. (c) High-resolution N 1s XPS of Ni-COF.

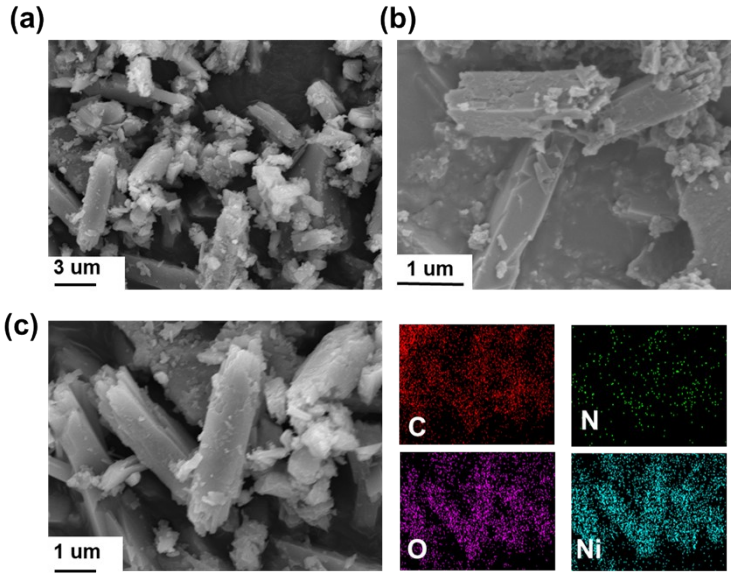


Figure S3. SEM image and the corresponding EDS elemental mappings of Ni-COF.

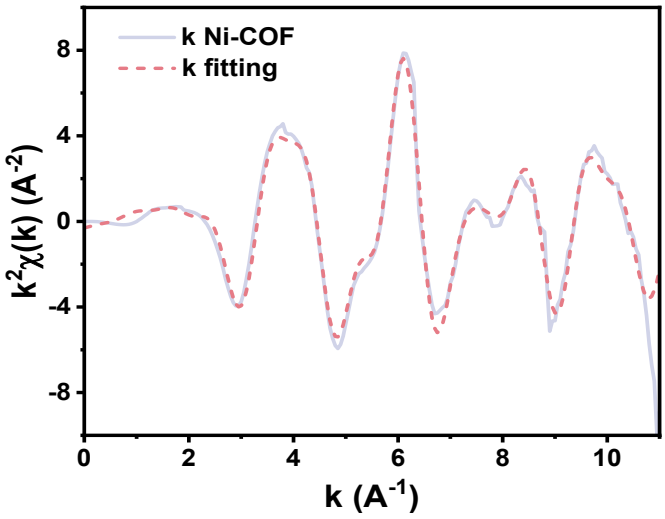


Figure S4. EXFAS fitting curves for Ni-COF.

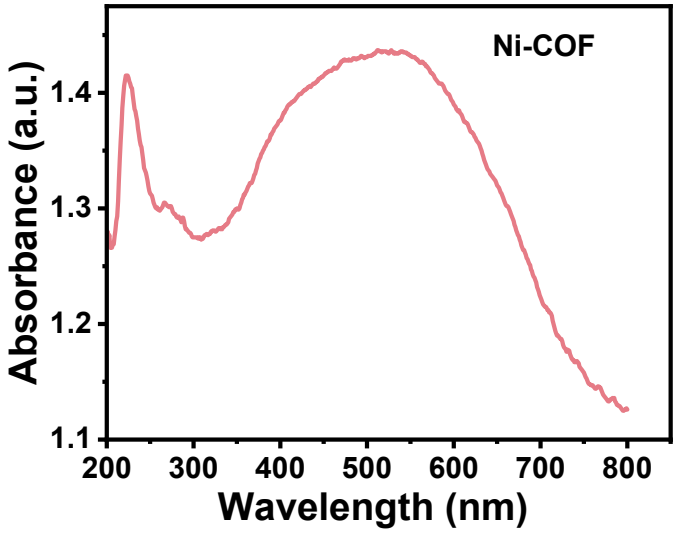


Figure S5. UV–vis spectra of Ni-COF.

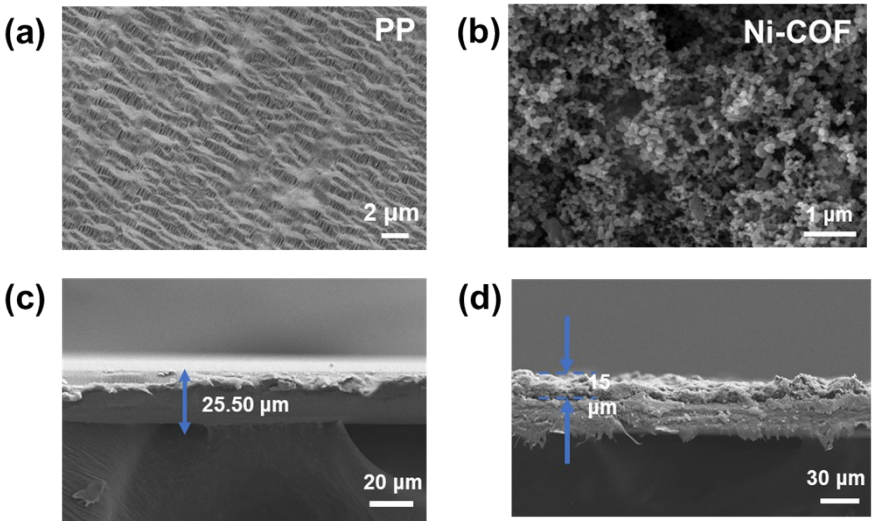


Figure S6. SEM images and cross-section SEM images of different separators.

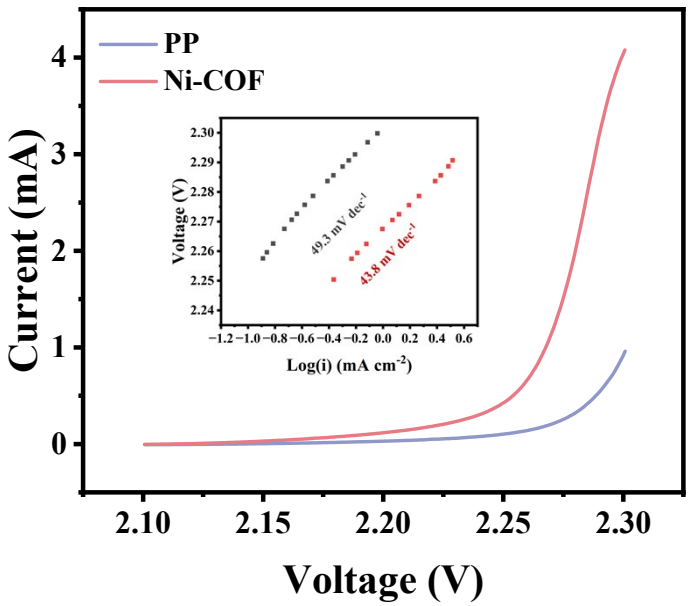


Figure S7. The Tafel plots calculated from the oxidative peaks in CV curves.

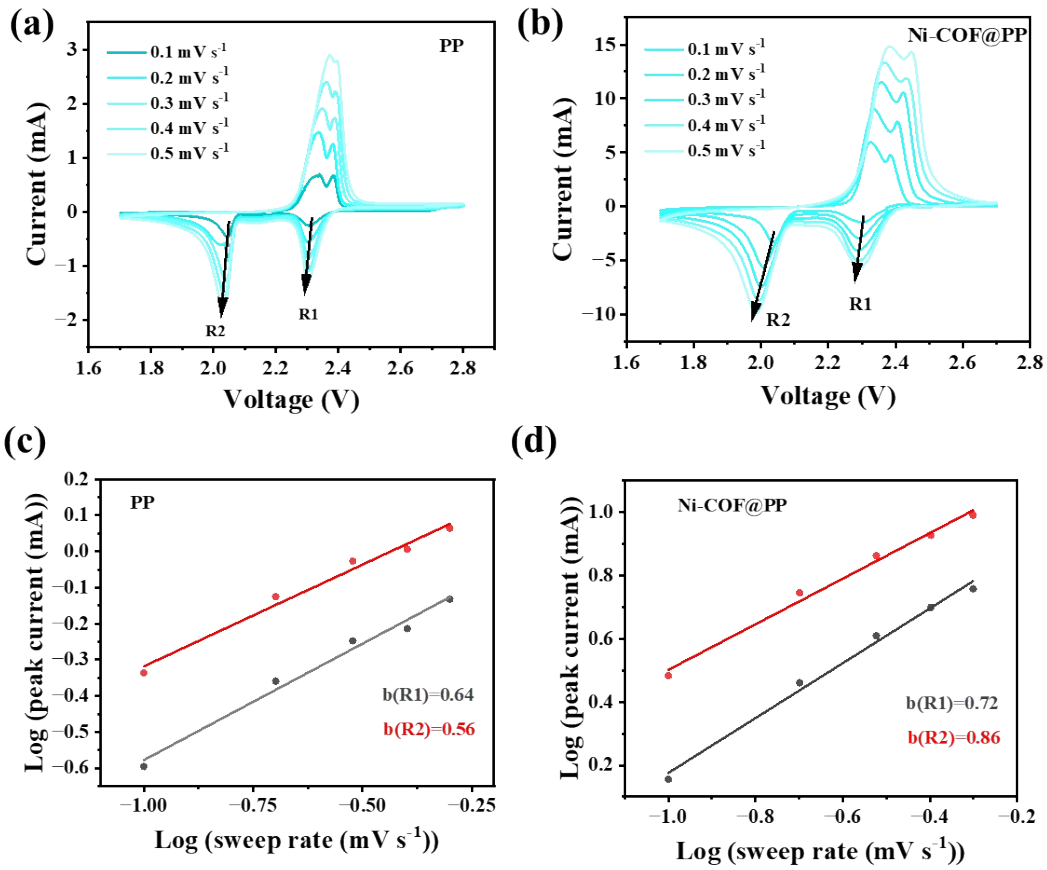


Figure S8. CV curves of the LSBs assembled with different (a) PP and (b) Ni-COF@PP. (c) The Linear fitting plot of peak current versus $v^{0.5}$ with PP and (d) Ni-COF@PP separators at reductive peak R1 and reductive peak R2.

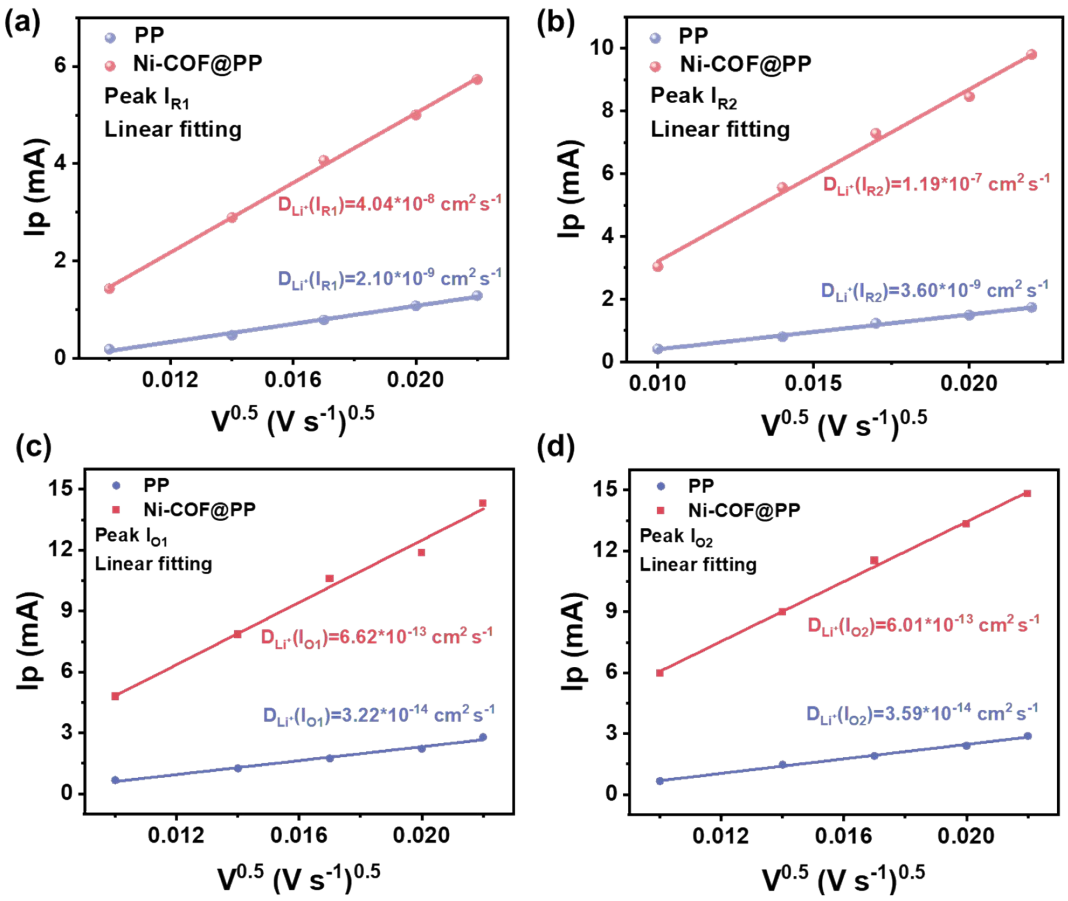


Figure S9. $Li^+$ diffusion coefficients ($D_{Li+}$) of various separators.

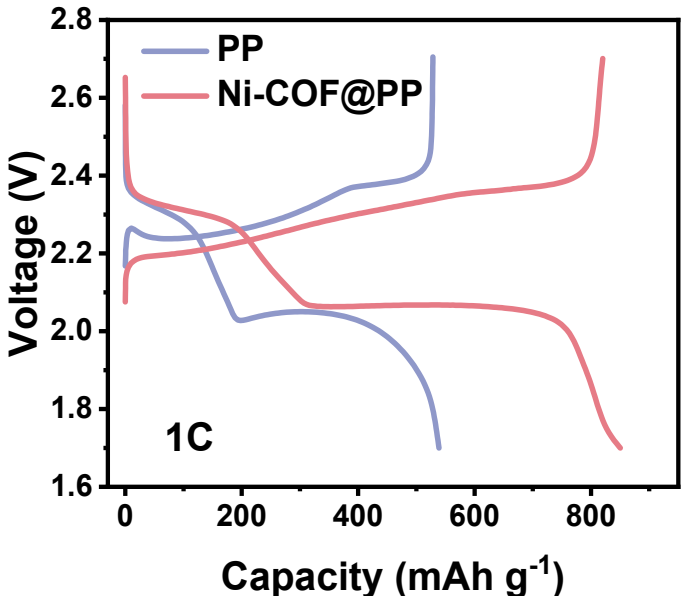


Figure S10. Galvanostatic discharge-charge profiles at 1 C of Li-S batteries with PP and Ni-COF@PP separators.

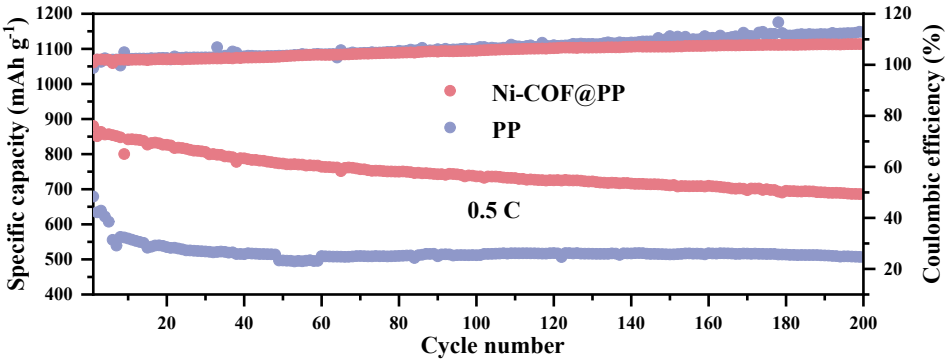


Figure S11. Cycling performance at 0.5 C over 200 cycles with PP and Ni-COF@PP separators.

As the cycle progresses, the Coulomb efficiency exceeds 100%. This can be ascribed to the loss of active sulfur upon cycling resulting from the shuttle effect. In addition, repeated volume changes of the sulfur cathode during cycling damage the cathode structure, further resulting in active sulfur loss and impacting CE[8-10].

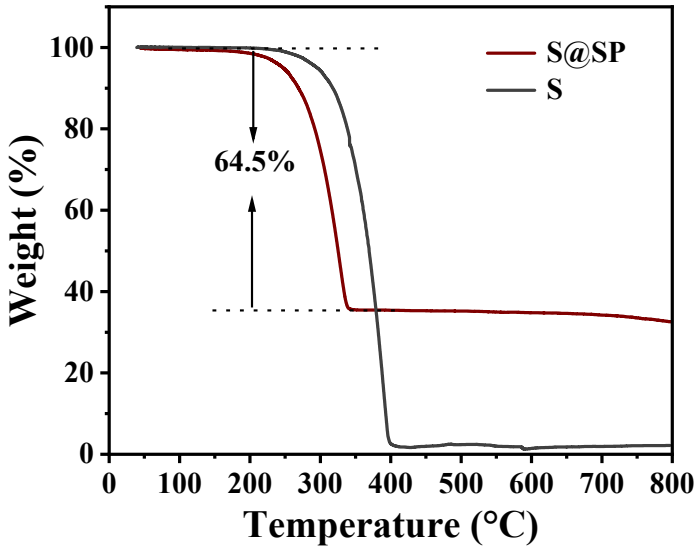


Figure S12. TGA curves of the S powder and S@SP compounds.

**Table S1.** Ni elemental analysis of Ni-COF.

| | Ni wt% (Calcd.) | Ni wt% (Tested) |
|---|---|---|
| **Ni-COF** | **22.72** | **25.72** |

## References


[1] a) G. Kresse, J. Furthmuller, *Phys. Rev. B* **1996**, 6, 15; b) S. Grimme, S. Ehrlich, L. Goerigk, *J. Comput. Chem.* **2011**, 32, 1456.

[2] J. P. Perdew, K. Burke, M. Ernzerhof, *Phys. Rev. Lett.* **1998**, 80, 891.

[3] P. E. Blöchl, *Phys. Rev. B* **1994**, 50, 17953.

[4] S. Grimme, J. Antony, S. Ehrlich, H. Krieg, *J. Chem. Phys.* **2010**, 132.

[5] H. J. Monkhorst, J. D. Pack, *Phys. Rev. B* **1976**, 13, 5188.

[6] P. J. Stephens, F. J. Devlin, C. F. Chabalowski, M. J. Frisch, *J. Phys. Chem.* **1994**, 98, 11623.

[7] M. Frisch, G. W. Trucks, H.B. Schlegel, G.E. Scuseria, M.A. Robb, J.R. Cheeseman,G. Scalmani, V. Barone, B. Mennucci, G. Petersson, *Gaussian 09, Rev. D 01* **2009.**

[8] Shunlong, J.; Jikai, Y.; Hongyu, Z.; Wenbin, W.; Guanglin, X.; Wengang, C.; Yaxiong, Y.; Hongge, P.; Xuebin, Y., Energy Storage Mater. 2023, 56, 1-12.

[9] Linhai, S.; Zhongping, L.; Lipeng, Z.; Hyunseok, M.; Cheng, S.; Kyeong-Seok, O.; Xiangtao, K.; Diandian, H.; Zhiqiang, Z.; Yang, W.; Sang-Young, L.; Liwei, M., Energy Storage Mater. 2024, 66, 103222.

[10] Geng, C.; Qu, W.; Han, Z.; Wang, L.; Lv, W.; Yang, Q. H., Adv. Energy Mater. 2023, 13 (15), 2204246.